RSC Advances

ROYAL SOCIETY OF CHEMISTRY

www.rsc.org/advances

Graphene: A Self-Reducing Template for Synthesis of Graphene-Nanoparticles Hybrids

M. Manolata Devi[1], Sumit Ranjan Sahu[1], Puspal Mukherjee[2], Pratik Sen[2] and Krishanu Biswas[1*]

[1]Department of Materials Science and Engineering, [2]Department of Chemistry, Indian Institute of Technology Kanpur, Kanpur-208016, U.P., India

Abstract: Integration of graphene with certain metallic nanoparticles, such as Au, Ag, Pt, Pd, Cu, etc., to produce new generation of hybrid materials is a field of intense research now-a-days. Graphene, being a single atomic layer thick sheet of hexagonally arranged sp^2 carbon atoms, has prodigious number of free electrons, which can be used to reduce metallic ions to produce the hybrid material consisting of metal nanoparticles on the 2D fabric of graphene. Efforts were made to explore such property of the virgin graphene by careful *in-situ* study using UV-visible (UV-vis) spectroscopy and transmission electron microscopy (TEM). The results indicate that it is possible to use surface potential of graphene to reduce Au^{3+}, Ag^{+}, Pt^{2+}, Pd^{2+} and Cu^{2+} ions to prepare graphene-metal nanoparticle hybrids. The extensive TEM studies substantiate the finding of the formation of graphene decorated with metal nanoparticles.

Keywords: Graphene, Metal nanoparticles, UV-visible spectroscopy, TEM, Hybrids

*Corresponding author, email: kbiswas@iitk.ac.in; Phone: +91-512-2596184; FAX: +91-512-2597505

1. Introduction

The graphene-metal (G-M) nanoparticle hybrids have attracted tremendous attention in the contemporary research due to their exceptional properties[1-6] and remarkable microstructures[7-9]. They can find potential applications in the field of nanoelectronics[10], composites[11,12], energy storage device[13-15], catalysis[16,17], transparent electrodes[18,19], sensors[20], biomedical applications[21] etc. The most remarkable aspect of decorating metallic nanoparticles on the 2D fabric of graphene is that the nanoparticles get directly decorated on the graphene nanosheets without the requirement of any molecular tag to bridge the graphene and the nanoparticles (NPs). The typical graphene sheet can be considered as an ideal substrate for dispersion of these nanoparticles because of the large active surface area per unit mass as compared to other forms of carbon e.g. nanotubes, amorphous carbon, graphite or diamond. However, the preparation of good quality hybrids with controlled size and morphology of the nanoparticles on the graphene sheets is of utmost importance for the various applications. The metal nanoparticles need to be uniformly distributed on the graphene sheets for the accomplishment of the desired properties[22-23]. These hybrids are usually prepared via chemical routes[18,24,25]. Usually, the precursors of different metal salts are reduced by a reducing agent in a solvent containing dispersed graphene oxide (GO) or reduced graphene oxide (RGO) nano platelets. One can use either two-step reduction of GO followed by metal salt or single step simultaneous reduction of mixture of GO and metal salt[24-26]. However, this requires careful process control to obtain homogeneous distribution of metal NPs on the graphene sheets. In addition, it requires a careful selection of the reducing agent to obtain the desire microstructure.

As graphene is made up of single atomic layer sheet of hexagonally arranged sp^2 bonded carbon atoms[1], it has large pool of π-electrons on its surface. Therefore, it is expected to

behave as a potential substrate for the reduction of metal ions and to be decorated uniformly on the graphene sheets. This would provide unique opportunity to decorate graphene nanosheets (G-Ns) with different metal nanoparticles. With this expectation, the present study is intended to probe this aspect of pristine graphene. Using Au^{3+}, Ag^{+}, Pt^{2+}, Pd^{2+} and Cu^{2+}, it would be seen whether these metal ions can be reduced by free electrons available on the G-Ns. It is to be noted that $Au^{3+}{}_{(1.50V),}$ $Ag^{+}{}_{(0.80V),}$ $Pt^{2+}{}_{(1.18V)}$ and $Pd^{2+}{}_{(0.951V)}$ have high reduction potential and it is expected that graphene can easily reduce these metal ions. However, Cu^{2+} is relatively difficult to reduce in aqueous solution, as it possesses relatively lower reduction potential (+0.34 V)[27].

2. Experimental Section

2.1 Materials: Graphite powder (100 mesh, 99.9995%), silver nitrate ($AgNO_3$, 99.9%), hydrogen tetrachloroaurate (III) hydrate ($HAuCl_4$, 99.9%), copper sulfate ($CuSO_4$, 99.9%) (Alfa Aesar, India), palladium chloride ($PdCl_2$), platinum chloride ($PtCl_4$), sodium nitrate ($NaNO_3$), potassium permanganate ($KMnO_4$), concentrated sulfuric acid (H_2SO_4), ammonia solution (NH_4OH), hydrazine hydrate solution (H_2NNH_2. H_2O) and hydrogen peroxide (H_2O_2) (Sigma Aldrich, India), were used for the preparation of graphene and hybrids. All the chemicals were used in the condition as received without further purification. The water used in all the experiments was purified through a Millipore system (Thermo Smart2 Pure).

2.2 Preparation of graphene (G) and graphene-metal nanoparticles hybrids:

Graphite oxide was prepared by modified Hummer's method[28]. Graphene oxide (GO) was obtained by ultrasonication of 0.01g of the synthesized graphite oxide powder in 100 mL of distilled water in a 250 mL round-bottom flask for 2h. The pH of the GO solution was adjusted to 10 by addition of 350 µL 25% ammonia solution. The graphene were prepared by a simple chemical reduction using hydrazine hydrate (NH_2-NH_2) (previously reported in ref.

25). For reduction of GO, 35 μL of hydrazine hydrate (NH_2-NH_2) was added slowly and the whole suspension was refluxed in an oil bath at 90^{o}C for 2h while stirring. To remove any residual hydrazine hydrate in the solution, the black coloured solution of graphene was heated (at 120^{o}C for 5h) above the reported boiling point of hydrazine hydrate (114^{o}C). Finally, completely dried black colored sheets of graphene are obtained. The graphene sheets are further dispersed in water and used as graphene stock solution.

To obtain graphene-metal hybrids, equal volume of graphene stock solution (20 mL) and aqueous solution of metal salts were mixed slowly to each other and heated at 90^{o}C for 15 min for each case. In case of Ag-G, equal volume (20 mL) of graphene stock solution and $AgNO_3$ aqueous solution (0.001M) were slowly mixed in a 250 mL round-bottom flask. The solution was heated to 90^{o}C while stirring for 15 min to complete the reaction. The solution was centrifuged several times with ethanol and water to obtain the desire dispersion. Similarly, the formation of Au-G, Cu-G, G-Pt and G-Pd were also achieved by reduction of $HAuCl_4$, $CuSO_4$, H_2PtCl_6 and H_2PdCl_4 (0.001 M) aqueous solution respectively in the graphene suspension.

2.3. *Characterization*

The specimens were extensively characterized using ultraviolet-visible (UV-vis) spectroscopy and transmission electron microscopy (TEM). The UV-vis absorption spectra were obtained in the range between 200 and 800 nm using a Jasco V-670 UV-vis spectrophotometer. The TEM images and selected area diffraction (SAD) patterns were acquired using FEI Tecnai G^2 U-twin instrument with accelerating voltage of 200 kV. TEM samples were prepared by adding few drops of the disperse solutions of sample in methanol on a 400 mesh size copper grids coated carbon film.

3. Results and Discussion

In the following, we shall describe and discuss the results of the present investigation. Firstly, we shall illustrate the formation of graphene-metal nanoparticles hybrids, characterized by different advanced techniques. This will be followed by detailed discussion on the *in-situ* UV-vis spectroscopic study to probe the formation of metal nanoparticles on the pristine graphene sheets. It is worthwhile to be noted that the resulting graphene after reduction has been characterized by Raman spectroscopy. The detailed analysis of the result (previously reported in ref. 25) indicated a significant red shift in the position of G band upon reduction of GO to graphene (from 1590 to 1579 cm^{-1}). The red shift of G band in graphene is mainly due to the restoration of conjugated sp^2-bonded C=C double during the reduction of GO[25]. This graphene solution has been further utilized for preparing G-M nanoparticles hybrid after complete removal of hydrazine hydrate so that the reduction of metal ions would be solely due to the surface potential of the graphene.

3.1 Microstructural Characterization

Figure 1(a-d) shows the bright field TEM images of different hybrids; Ag-G, Au-G, Cu-G and Pd-G, respectively. The figures reveal lamellar graphene sheets showing crumpled silk veil waves morphology. The metal (Ag, Au, Cu and Pd) nanoparticles (NPs) appear as black dots, uniformly distributed on the graphene sheets.

To confirm the presence of the metals NPs, selected area diffraction (SAD) patterns have been obtained. The SAD patterns of Ag-G (fig. 1(a) top inset), Au-G (fig.1 (b) top inset), Cu-G (fig.1(c) top inset) and Pd-G (fig.1 (d) top inset) reveals two prominent bright filed rings indicating polycrystalline nature of the graphene. These prominent rings are due to (002) and (100) planes of graphene. The sharp spotty rings in each SAD patterns of Ag-G, Au-G, Cu-G and Pd-G correspond to (111), (200), (220) and (311) planes of each metal (Ag, Au, Cu and Pd) nanoparticles. The bottom inset of each figure shows the histogram of particle size

distribution of Ag, Au, Cu and Pd nanoparticles, indicating the average particle size of Ag, Au, Cu and Pd to be 22 ± 3, 7 ± 3, 6 ± 2 and 8 ± 2 nm, respectively. The detailed TEM investigation, thus clearly demonstrates the formation of metal NPs on the pristine graphene nanosheets. In addition, it can clearly be observed that the metal nanoparticles are uniformly decorated on graphene surface. In order to control the size of the nanoparticle, the factors influencing the particle size such as concentration of the metal salts (≤0.001M), reaction time and temperature (15min and 90°C), high heating and cooling rate (≥ 10°C), slow rate of mixing of the reactant solutions have been utilized (see supporting information).

3.3 **Optical characterization**

In order to probe the reduction of metal ions to metal nanoparticles, extensive *in-situ* UV-vis spectroscopic studies have been carried out. Au, Ag, Pd and Cu nanoparticles are reported to exhibit surface plasmon resonance (SPR) in the wavelength range between 200 to 800 nm. Therefore, the evolution of the SPR peaks during the *in-situ* UV-vis spectroscopy was tracked and UV-Vis spectra were collected in definite time interval and compared. Figures 2 shows the UV-vis spectra of GO, G, Ag-G, Au-G, Cu-G and Pd-G. The UV-visible absorption spectrum of GO (Figure 2) shows an absorption peak at 230 nm, corresponding to the $\pi \rightarrow \pi^*$ transition of the aromatic π electrons and a small shoulder at 303 nm due to $n \rightarrow \pi^*$ transition of the C=O bonds[29]. However, for graphene (Figure 2), a peak is observed at 266 nm, corresponding to the $\pi \rightarrow \pi^*$ transition of the aromatic moiety. This red shift in the $\pi \rightarrow \pi^*$ absorption peak of graphene from 230 nm to 266 nm indicates the increase in the number of conjugated C=C double bonds. Thus, the π electronic conjugation has been restored within the graphene sheets after reduction. The shoulder at 303 nm disappears, indicating the formation of pristine graphene. UV-vis absorption spectrum of Ag-G (Figure 2) indicates two peaks; first one is due to graphene ($\pi \rightarrow \pi^*$ at 264 nm) and the second one is because of SPR peak of Ag NPs (at 418 nm). Similarly, absorption spectra of Au-G, Cu-G and Pd-G reveal

SPR peaks at 555, 540 and 368 nm for Au, Cu and Pd NPs respectively (see figure 2), in addition to the graphene peaks. The detailed peak positions are listed in Table I.

In the following, the results of the *in-situ* studies of UV-vis spectroscopy have been discussed. Figures 3(a-d) describe the results of Ag-G, Au-G, Cu-G and Pd-G respectively. It is to be noted that *in-situ* study allows us to obtain a large number of spectra at definite time interval. However, we shall show the salient spectra for clarity. In case of Ag-G (Figure 3a), as $AgNO_3$ solution has been added to graphene in the cuvette, a broad plasmon peak due to SPR of Ag NPs appears at 418 nm (within couple of minutes after addition). The peak remains at the same position for long time (1 day). The plasmon peak becomes quite sharp and prominent after 7 days. This observation strongly suggests that the π-electrons available on the graphene nanosheets can reduce Ag^+ to Ag NPs. UV-vis absorption spectrum of $AgNO_3$ aqueous solution is also shown in figure 3a for reference, which further confirms the SPR peak at 418 nm, is due to Ag NPs. Similarly, when $HAuCl_4$ aqueous solution has been added to graphene, a broad plasmon peak at 555 nm appears. This peak is due to SPR of Au NPs. Subsequent measurements reveals that the peak position does not change after 15 minutes of the reaction. The UV-vis absorption spectrum of $HAuCl_4$ aqueous solution is shown in figure 3b as reference. Similar finding have been made for Cu NPs (figure 3c) and Pd NPs (figure 3d) when corresponding aqueous solution have been added. It is to be noted that due to relatively lower reduction potential (+0.34 V) of Cu^{2+} ions as compared to the other metal ions, they are more prone to oxidized. Hence, the broad peak at 795 nm has been appeared in addition to the SPR peak of Cu NPs at 545 nm, which is due to formation of Cu_2O[30]. The experimental results clearly indicate that graphene surface can act as reducing agents for different metal ions to form metal NPs. A schematic diagram illustrating the reduction of metal ions by graphene is shown in figure 4.

In order to get confirm the formation of hybrids between the graphene and metal nanoparticles rather than a physical mixture, metal (Ag, Au, Cu and Pd) nanoparticles were separately prepared and the SPR peak positions were identified using UV-Vis spectroscopy. The SPR peak position of pure Ag, Au, Cu and Pd nanoparticles has been found to be at 431, 522, 518 and 384 nm respectively (see supporting information). One can clearly observed that the SPR peak position of metal nanoparticles are shifted after incorporation these nanoparticles with graphene due to charge transfer between nanoparticles and graphene[31], suggesting the formation of graphene-metal nanoparticles hybrids. The graphene-metal hybrids have been found to be highly stable in terms of particle size as a function of reaction time, temperature and reaction between graphene and metal nanoparticles (see supporting information). The particle sizes of nanoparticles in hybrids do not grow significantly as a function of time and temperature. Moreover, graphene has been reported to be highly stable toward those metals (Fe, Co, Ni etc.), which are very prone to form carbide with carbonaceous materials. It has been reported that these metal nanoparticles can be uniformly decorated on graphene surface without forming any carbides[32-34]. This clearly suggests that the graphene surface can be used as an ideal substrate for decoration of metal nanoparticles without forming any kind of by-products like carbides.

Graphene, being 2D materials, exhibits unique electronic properties, such as absence of charge localization, half-integer quantum Hall-Effect as well as ultra high mobility[35,36]. The electronic properties of graphene are primarily due to π- electrons, making it an example of perfect 2D system in which π-states form the valence band and π* states form the conduction band. The conduction electrons in graphene show remarkable electrical, optical as well as ballistic transport and high carrier mobility[35,36]. Thus, the presence of the large number of free electrons makes pristine graphene an ideal substrate for dispersion of the nanoparticles due to its large active surface. However, it is to be noted that the reduction potential of

graphene has been reported to be +0.38 V[37]. Thus, this process can be extended only for those metal ions whose reduction potential is higher than that of graphene.

4. Conclusions

The immense potential of graphene can effectively be realized by producing different hybrids. The most notable one is graphene-metal NPs hybrids; showing potentials for many application. In contrast to the conventional accepted methodology for preparation of these hybrids, the present investigation reports, for first time, that surface potential of pristine graphene can effectively be utilized to prepare these hybrids. Using *in-situ* UV-vis spectroscopy coupled with TEM, it has categorically shown that Au^{3+}, Ag^{+}, Pd^{2+} and Cu^{2+} ions are reduced on the virgin RGO surface to obtain homogeneous distribution of the NPs on the RGO surface.

In the present investigation, graphene, obtained as reduced graphene oxide (RGO) is made from GO by chemical reduction. It is well known that this reduction process removes the oxygen-containing functional group from the basal plane and edges of the GO sheets[38]. Normally, these oxygen containing groups such as carbonyl (-C=O), epoxy (-O-), carboxyl (-COOH), and hydroxyl (-OH) group act as inhibitor for electron transfer. Thus, virgin RGO surface is deemed to be conducive for electron transfer for reduction of various metal ions. Thus, in absence of these groups, metal ions can be easily reduced and the hybrids can be obtained by anchoring these NPs to the surface of the graphene or RGO through covalent or even non-covalent bonding[39]. Previous reports show that G-M hybrids can be produced using chemical linkers having strong affinity towards graphene surface *via* stacking[8,9]. The present investigation categorically reveals that, G-M hybrids can be synthesized without using any linker.

ACKNOWLEDGEMENT

This work was supported by research funding from Department of Science and Technology (DST), Government of India. The authors would like to acknowledge the usage of Transmission Electron Microscopy facility at IIT Kanpur.

References

1. A. K. Geim and K. S. Novoselov, *Nat. Mater.* 2007, **6**, 183-191.
2. X. Huang, Z. Yin, S. Wu, X. Qi, Q. He, Q. Zhang, Q. Yan, F. Boey and H. Zhang, *Small* 2011, **7***,* 1876-1902.
3. C. Lee, X. Wei, J. W. Kysar and J. Hone, *Science* 2008*,* **321**, 385–388.
4. A. A. Balandin, S. Ghosh, W. Bao, I. Calizo, D. Teweldebrhan, F. Miao and C.N. Lau, *Nano Lett.* 2008*,* **8**, 902–907.
5. K. I. Bolotin, K. J. Sikes, Z. Jiang, M. Klima, G. Fudenberg, J. Hone, P. Kim and H. L. Stormer, *Solid State Commun.* 2008*,* **146**, 351–355.
6. M. D. Stoller, S. Park, Y. Zhu, J. An and R. S. Ruoff, *Nano Lett.* 2008, **8**, 3498–3502.
7. J. C. Meyer, A. K. Geim, M. I. Katsnelson, K. S. Novoselov, T. J. Booth and S. Roth, *Nature* 2007, **446,** 60-63.
8. J.M. Englert, C. Dotzer, G. Yang, M. Schmid, C. Papp, J. M. Gottfried, H.P. Streinruck, E. Spiecker, F. Hauke and A. Hirsch, *Nat. Chem*. 2011, **3**, 279-286.
9. S. Guo, S. Dong and E. Wang, *ACS Nano* 2010, **4**, 547-555.
10. D. A. Areshkin and C. T. White, *Nano Lett*. 2007, **7**, 3253–3259.
11. S. Stankovich, D. A. Dikin, G. H. B. Dommett, K. M. Kohlhaas, E. J. Zimney, E. A. Stach, R. D. Piner, S. T. Nguyen and R. S. Ruoff, *Nature* 2006, **442**, 282-286.
12. U. Khan, P. May, A. O'Neill and J. N. Coleman, *Carbon* 2010, **48**, 4035–4041.
13. M. D. Stoller, S. Park, Y. Zhu, J. An and R. S. Ruoff, *Nano Lett.* 2008, **8**, 3498–3502.

14. S. Chu, L. Hu, X. Hu, M. Yang and J. Deng, *Int. J. Hydrogen Energy* 2011, **36**, 12324-12328.

15. T. Lu, L. Pan, H. Li, G. Zhu, T. Lv, X. Liu, Z. Sun, Ting Chen and D. H.C. Chua, *J. Alloys Compd.* 2011, **509**, 5488–5492.

16. H. Zhang, X. Xu, P. Gu, C. Li, P. Wu and C. Cai, *Electrochim. Acta* 2011, **56**, 7064–7070.

17. A.R. Siamaki, A. E. R.S. Khder, V. Abdelsayed, M. S. E. Shall and B. F. Gupton, *J. Catal.* 2011, **279**, 1–11.

18. S. Wang, S.P Jiang and X. Wang, *Electrochim. Acta* 2011, **56**, 3338–3344.

19. A.M. Shanmugharaj, W.S. Choi, C.W. Lee and S. H. Ryu, *J. Power Sources* 2011, **196**, 10249–10253.

20. F. Schedin, A. K. Geim, S. V. Morozov, E. W. Hill, P. Blake, M. I. Katsnelson and K. S. Novoselov, *Nat. Mater*. 2007, **6**, 652–655.

21. B. D. Gusseme, L. Sintubin, L. Baert, E. Thibo, T. Hennebel, G. Vermeulen, M. Uyttendaele, W. Verstraete and N.Boon, *Appl. Environ. Microbiol*. 2010, **76**, 1082-1087.

22. V. Singh, D. Joung, L. Zhai, S. Das, S.I. Khondaker and S. Seal, *Prog. Mater Sci*. 2011, **56**, 1178–1271.

23. K. S. Subrahmanyam, A. K. Manna, S. K. Pati and C. N. R. Rao, *Chem. Phys. Lett.* 2010, **497**, 70–75.

24. Z. Xu, H. Gao and H. Guoxin, *Carbon* 2011, **49**, 4731-4738.

25. S. R. Sahu, M. M. Devi, P. Mukherjee, P. Sen and K. Biswas, *J. Nano Mat.* 2013, **2013**, 1-9.

26. W. Yuana, Y. Gua and L. Li, *Appl. Surf. Sci.* 2012, **261**,753-758.

27. Y. Wan, X. Wang, H. Sun, Y. Li, K. Zhang and Y. Wu, *Int. J. Electrochem. Sci.,* 2012**,** **7**, 7902 – 7914.

28. W. S. Hummers and R. Offeman, *J. Am. Chem. Soc.* 1958**, 80**, 1339.

29. T. T. Dang, V. H. Pham, S. H. Hur, E. J. Kim, B. S. Kong and J. S. Chung, *J. Colloid Interface Sci.* 2012, **376**, 91-96.

30. S. H. Wu and D.H. Chen, *J. Colloid Interface Sci.* 2004, **273**, 165-169.

31. M. M. Devi, S. R. Sahu, P. Mukherjee, P.Sen and Krishanu Biswas, *Trans. IIM*, 2015; DOI 10.1007/s12666-015-0566-0.

32. M. Gaboardi, A. Bliersbach, G. Bertoni, M. Aramini, G. Vlahopoulou, D. Pontiroli, P. Mauron, G. Magnani, G. Salviati, A. Z¨uttel and M. Ricc`o, *J. Mater. Chem. A*, 2014, 2, 1039–1046.

33. Y. Li, Z. Zhou, G. Yu, W. Chen and Z. Chen, *J. Phys. Chem. C 2010*, 114, 6250–6254.

34. S. Naji, A. Belhaj, H. Labrim, M. Bhihi, A. Benyoussef, and A. El Kenz, *J. Phys. Chem. C* 2014, 118, 4924−4929.

35. E. L. Wolf, *Graphene: A New Paradigm in Condensed Matter and Device Physics*, Oxford University Press*,* UK. 2013.

36. O. V. Yazyev and S. G. Louie, *Nat. Mater*. 2010, **9**, 806-809.

37. B. S. Kong, J. Geng and H. T. Jung, *Chem. Commun*., 2009, 2174–2176; DOI: 10.1039/b821920f

38. X. Gao, J. Jang and S. Nagase, *J. Phys. Chem. C* 2010, **114**, 832–842.

39. V. Georgakilas, M. Otyepka, A. B. Bourlinos, V. Chandra, N. kim, K. C. Kemp, P. Hobza, R. Zboril and K. S. Kim, *Chem. Rev*. 2012, **112**, 6156-6214.

List of Figure files

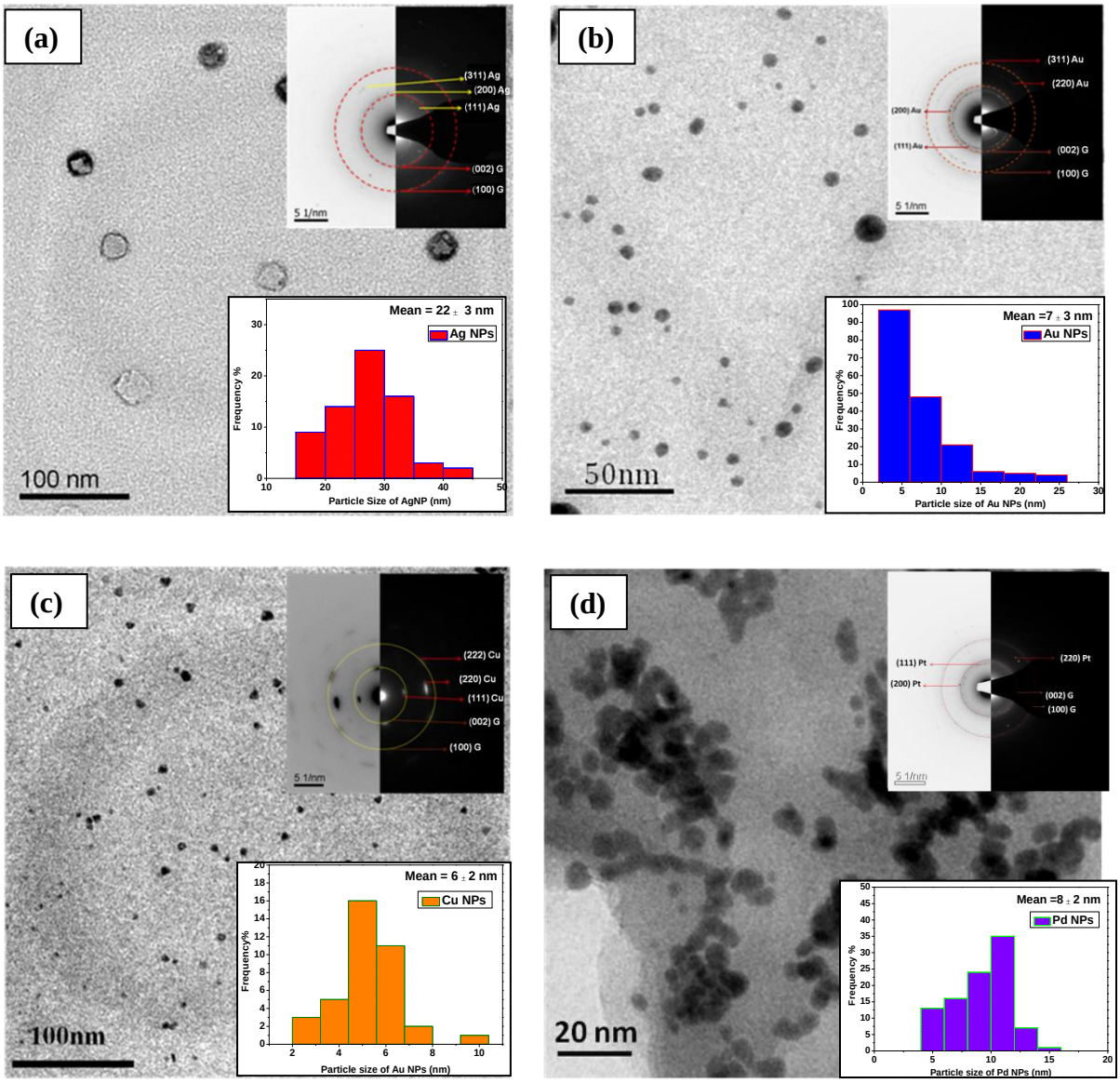

Figure 1: TEM micrographs and corresponding SAD patterns of (a) Ag-G, (b) Au-G, (c) Cu-G and (d) Pd-G. The upper inset in each figure shows SAD pattern whereas lower inset shows nanoparticles size distribution.

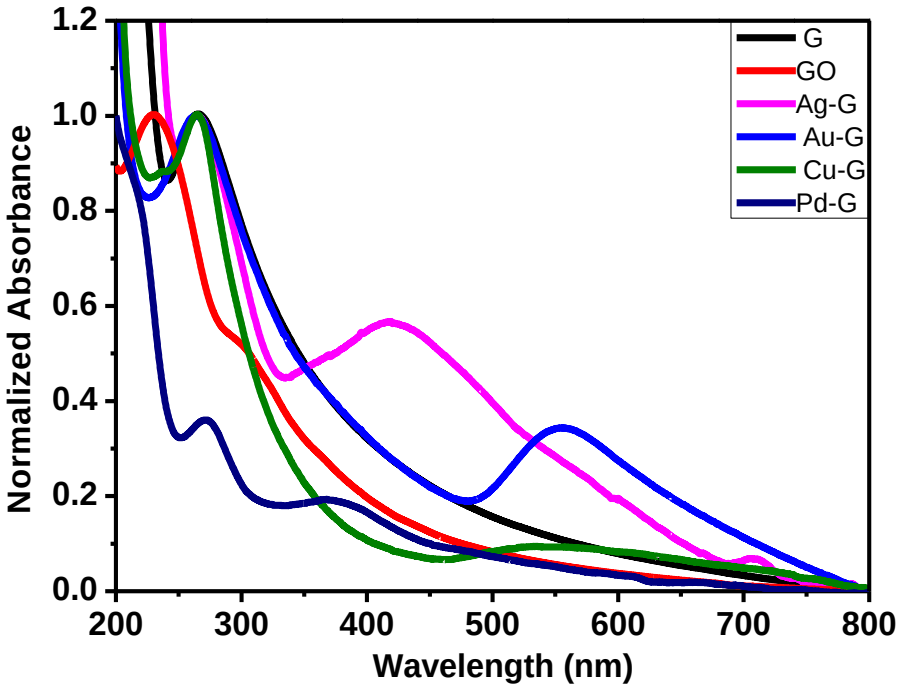

Figure 2: Absorbance spectra of different samples using UV-vis spectroscopy.

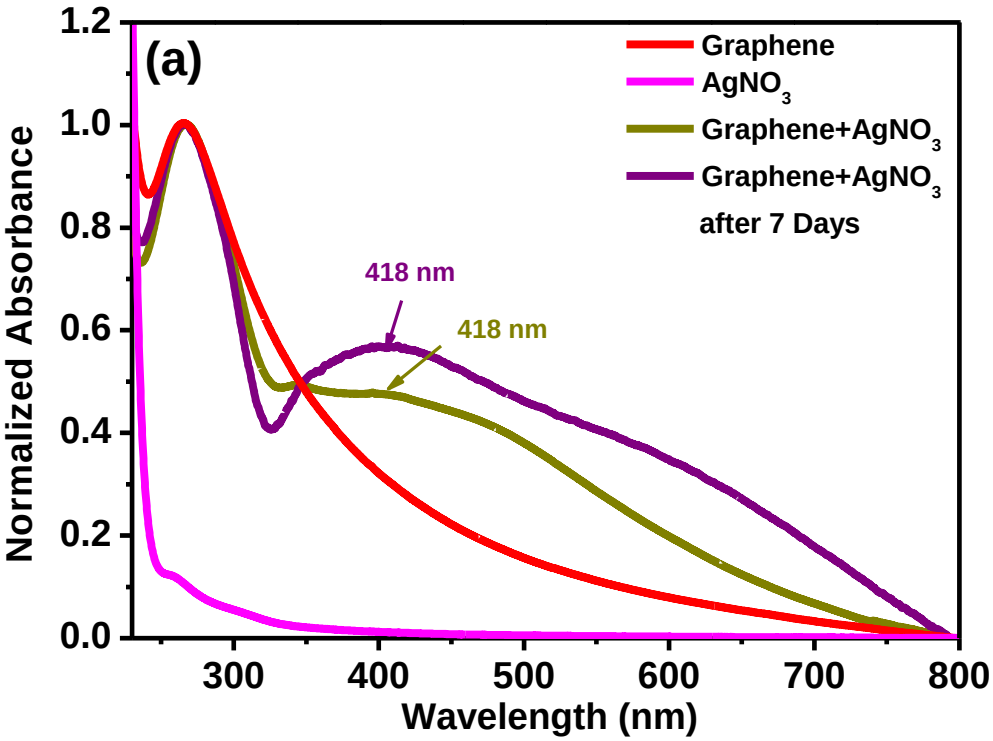

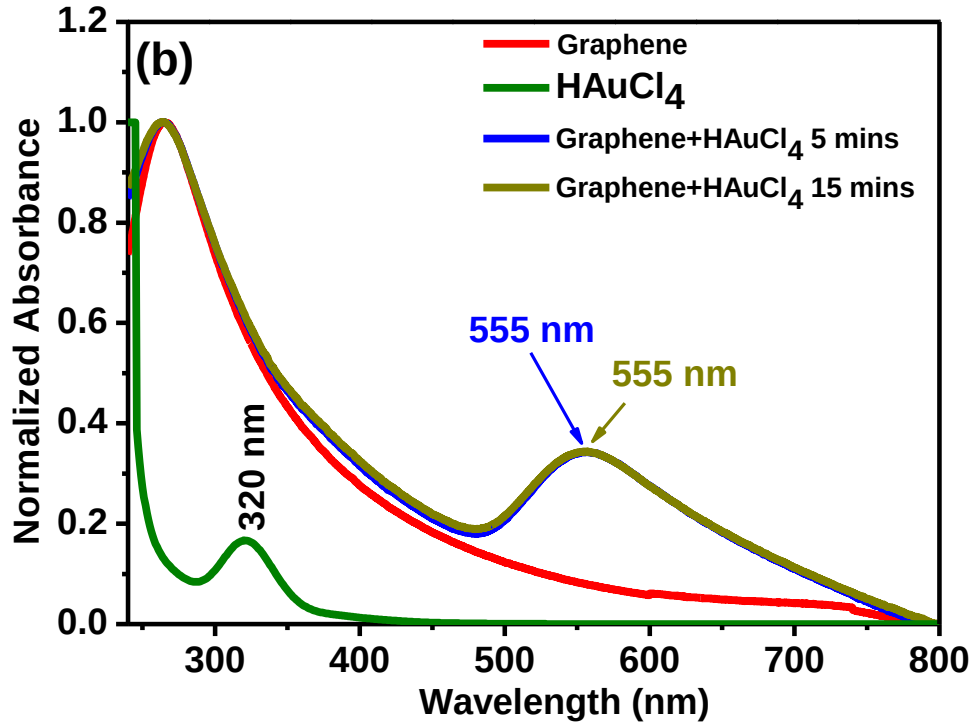

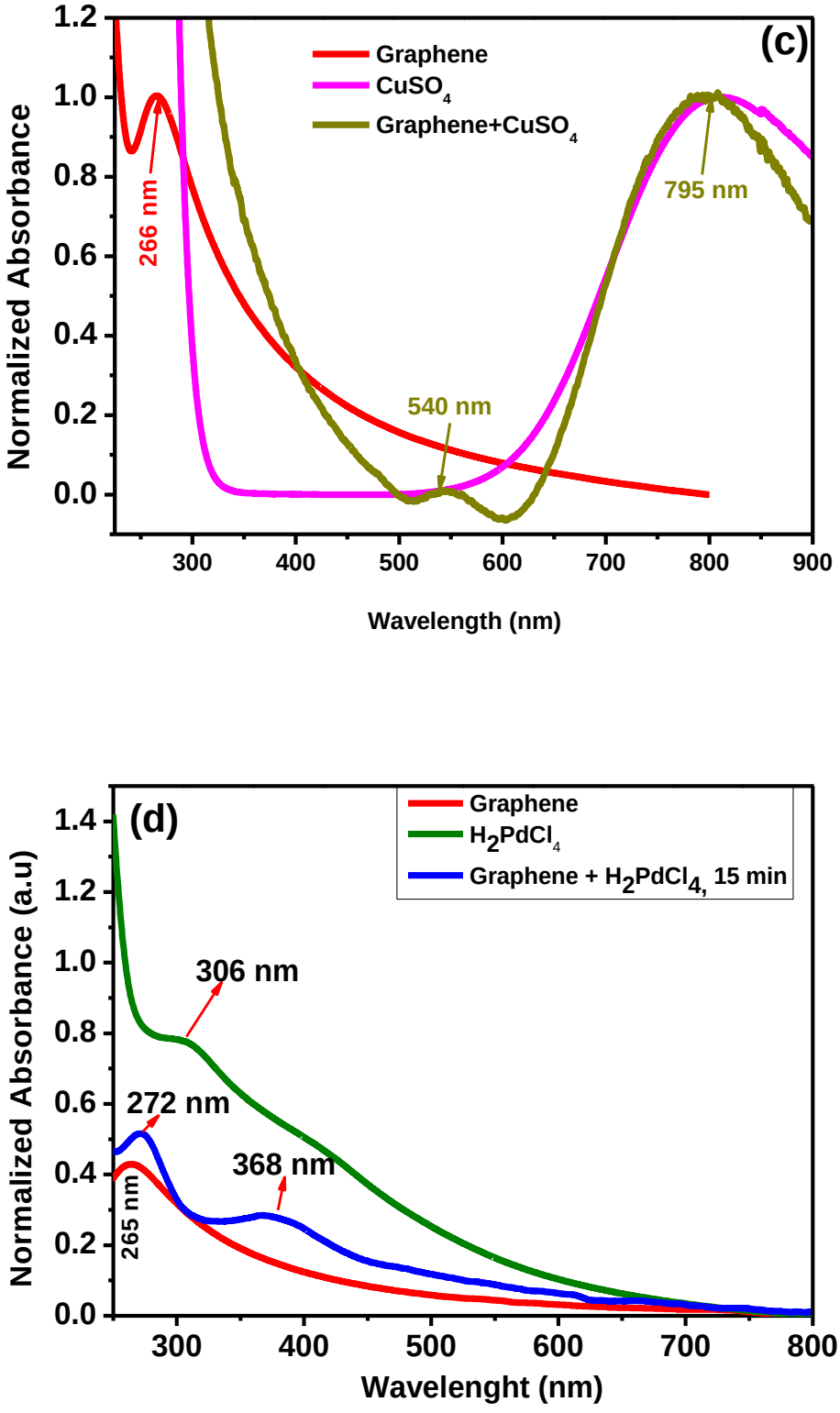

Figure 3: Results of *in-situ* UV-visible spectroscopy: (a) Ag-G; (b) Au-G; (c) Cu-G and (d) Pd-G.

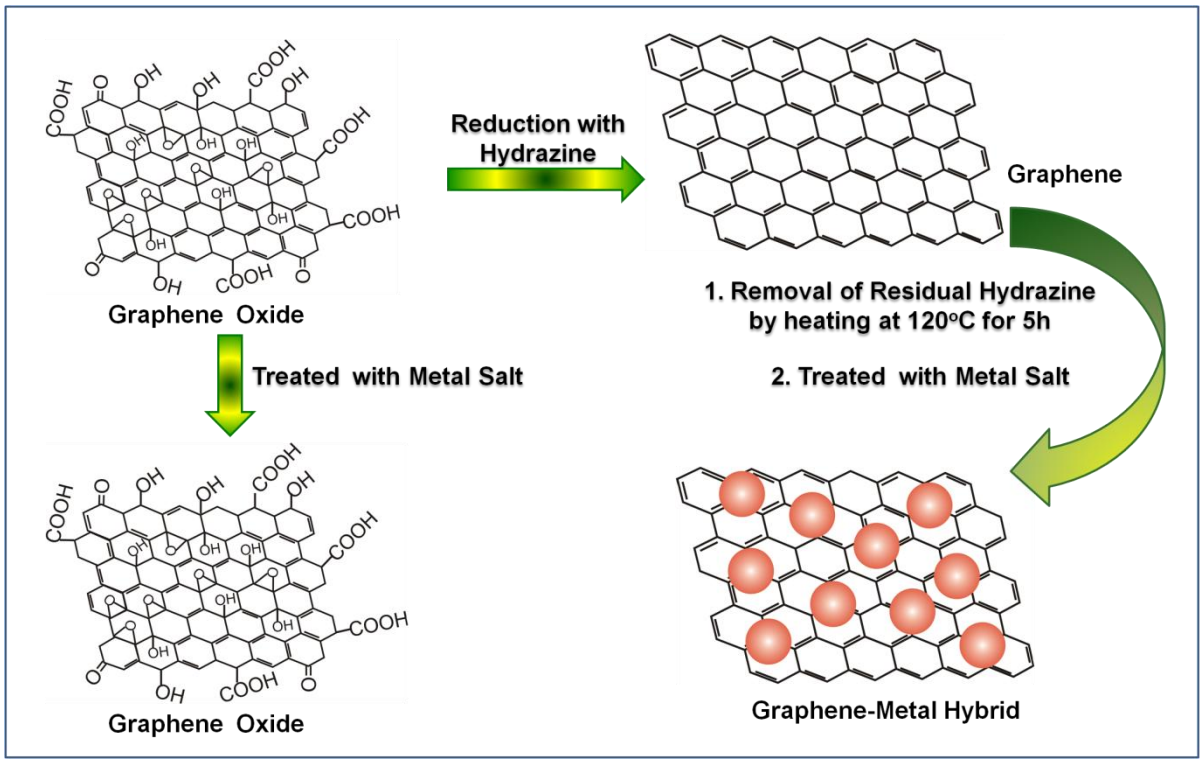

Figure 4: A schematic diagram illustrating the reduction of metal ions by graphene without any reducing agent whereas graphene oxide could not reduce metal ions.

List of Table

Table I. Comparison of UV-visible peak positions of GO, G, metal (Ag, Au, Cu and Pd) NPs and Metal – Graphene (Ag-G, Au-G, Cu-G and Pd-G) Hybrids.

Material	G Peak Position	SPR Position
GO	230 and 303 nm	---
Graphene (G)	266 nm	---
Ag NPs	---	431 nm
Ag-G Hybrid	265 nm	418 nm
Au NPs	---	522 nm
Au-G Hybrid	260nm	555 nm
Cu NPs	---	518 nm
Cu-G Hybrid	265 nm	540 nm
Pd NPs	---	384 nm
Pd-G Hybrid	265 nm	368 nm